# Self-consistent Gorkov-Green's function method for semimagic nuclei:
# Perturbation theory for the polarization propagator with the algebraic diagrammatic construction

**Gianluca Stellin**[1,2,3], **Vittorio Somà**[2] and **Thomas Duguet**[2,4]

[1] Cnrs, IJCLab, Bât. 100, 15 Rue Georges Clemenceau, 91405 Orsay, France.
[2] DRF/DPhN/Irfu/LENA, CEA Paris Saclay and Université Paris-Saclay, 91191 Gif-sur-Yvette, France.
[3] Espace de Structure et de réactions Nucléaires Théorique, CEA Paris-Saclay, Bât. 703, 91191 Gif-sur-Yvette, France.
[4] Department of Physics and Astronomy, Instituut voor Kern- en Stralingsfysica, KU Leuven, 3001 Leuven, Belgium.

## State of the art

*Ab-initio* self-consistent Gorkov-Green's function theory (SCGGF) avails of an efficient approximation scheme for the nuclear wavefunctions, the correlation-expansion method, entailing a *polynomial scaling* $\propto M^{\alpha}$ with $\alpha \geq 4$ in the size $M$ of the space of single-particle excitations. The wavefunctions are constructed by building particle-hole excitations on top of a reference state by means of a correlator. For open-shell nuclei, reference states with a fixed particle number $A$ are almost degenerate with respect to the excitation of nucleons to the adjacent single-particle energy level.

▶ In SCGGF theory for *semi-magic* nuclei, this degeneracy is lifted by breaking the symmetry associated to particle-number, that corresponds to the $\mathrm{U}(1)_Z \times \mathrm{U}(1)_N$ symmetry group [1], in the reference ground state on top of which perturbation theory is applied. This approach counts a number of applications, including binding energies, charge radii, one and two-nucleon separation energy [2, 3], two neutron shell gaps [4] and charge radii [5, 6] and charge-density distribution [7, 8] of even-even nuclei as well as low-lying excited states [5], neutron addition and removal spectral distribution of odd nuclei [3, 5, 9].

▶ Self-consistent perturbation theory the one-body Gorkov-Green's functions includes two and three-body forces, in the ADC(2) approx. scheme [10]. The formalism for the ADC(3) has been derived [11], but not yet implemented. For doubly open-shell nuclei, the breaking of the symmetry associated with total angular momentum, $\mathrm{SU}(2)$, which entails the inclusion of deformation in the reference state, is more congenial [12].

## Theoretical framework

Operators representing physical observables are expressed in terms of second-quantization operators, carrying a single particle index, $b \equiv (n, \ell, j, m, q)$, where $n$ is the principal quantum number, $\ell$ is the orbital angular momentum, $j$ is the total angular momentum and $m$ ($q$) is the $z$-projection of the total angular momentum (isospin).

▶ The Hilbert space associated with a single-nucleon $\mathscr{H}_1$ is split into two blocks, characterized by the opposite sign of the total angular momentum projection along the $z$ axis. The two partitions of $\mathscr{H}_1$ constitute a 2D vector space, the Nambu space [1, 13, 14].

▶ The partitions are labeled by a Nambu index $g = 1, 2$ and are mapped one another by means of *time reversal*, corresponding to the *involution* in single-particle space, $b \mapsto \bar{b}$. Hence, involuted *creation*, $a^{\dagger}_{\bar{b}} \equiv \eta_b a^{\dagger}_{\tilde{b}}$, and *annihilation* operators, $a_{\bar{b}} \equiv \eta_b a_{\tilde{b}}$, are introduced, where $\tilde{b} \equiv (n, \ell, j, -m, q)$ and the phase factor $\eta_b = (-1)^{\ell - j - m}$ is real, such that $\eta_b \eta_{\tilde{b}} = -1$ and $\eta_b \eta^{*}_b = \eta^2_b = 1$.

▶ The second-quantization operators are rearranged into two rank-one tensors,

$$\mathbf{A}_a \equiv \begin{pmatrix} a_a \\ \bar{a}^{\dagger}_a \end{pmatrix}, \quad \mathbf{A}^{\dagger}_a = \begin{pmatrix} a^{\dagger}_a & \bar{a}_a \end{pmatrix},$$

and $\mathbf{A}^{*}_a \equiv (\mathbf{A}^{\dagger}_a)^T$, obeying the canonical anticommutation rules [15]. The *involution* in Nambu space is also defined, with the rule $\bar{g} = 1\,(2)$ if $g = 2\,(1)$.

▶ The system is described by the grand-canonical potential,

$$\Omega = \overbrace{T + U - \mu_n N - \mu_p Z}^{\Omega_U} + \overbrace{V^{\mathrm{NN}} - U}^{\Omega_I},$$

where $T$, the *kinetic energy* operator with $t_{ab} \equiv (a|T|b)$, is expressed as

$$T = \sum_{ab} t_{ab}\, a^{\dagger}_a a_b\,,$$

and $V^{2\mathrm{N}}$ is partially antisymmetrized *two-body potential energy* operator,

$$V^{2\mathrm{N}} = \sum_{\substack{ab \\ cd}} \frac{1}{(2!)^2}\, \bar{v}_{abcd}\, a^{\dagger}_a a^{\dagger}_b a_d a_c\,,$$

with $\bar{v}_{abcd} \equiv \big[(ab|V^{2\mathrm{N}}|cd) - (ab|V^{2\mathrm{N}}|dc)\big]$, and $U$ is the *one-body potential energy* operator,

$$U = \frac{1}{2}\sum_{ab}[u^{11}_{ab}\, a^{\dagger}_a a_b + u^{22}_{ab}\, a_{\bar{a}} a^{\dagger}_{\bar{b}} + u^{12}_{ab}\, a^{\dagger}_a a^{\dagger}_{\bar{b}} + u^{21}_{ab}\, a_{\bar{a}} a_b]\,,$$

explicitly breaking particle-number symmetry, $\mathrm{U}(1)_Z \times \mathrm{U}(1)_N$ [16].

▶ The expansion scheme exploits a reference state that builds the correlated state on top of a Bogoliubov vacuum, accounting for static pairing correlations. Nonetheless, the exact ground state (*g.s.*) of $\Omega$ does preserve $\mathrm{U}(1)_Z \times \mathrm{U}(1)_N$ symmetry. Moving away from semimagic nuclei, SCGGF theory becomes less effective. Significant quadrupole correlations, *i.e.* static deformation, spoil the agreement with the experimental data, thus SU(2)-breaking reference states are preferred in that context [12].

▶ Starting from $\Omega$, one introduces the *modified Heisenberg* (cf. $\mathbf{A}_b(t)$ and $\mathbf{A}^{\dagger}_b(t)$) and *interaction picture* for the time evolution of the second quantization operators (cf. $\mathbf{A}_{I\,b}(t)$ and $[\mathbf{A}_{I\,b}(t)]^{\dagger}$).

## Diagrammatic expansion

Let us consider the perturbative expansion of the Nambu components of the polarization propagator in terms of $\Omega_I$. The master formula is expressed in terms of the second quantization operators in the interaction picture (cf. Ref. [19] for SCGF theory),

$$\Pi^{g_1 g_2 g_3 g_4}_{acdb}(t, t^{+}, t'^{+}, t') = -i\sum_{l=0}^{+\infty}\left(\frac{-i}{\hbar}\right)^l \frac{1}{l!}\int_{-\infty}^{+\infty}\mathrm{d}t_1 \ldots \int_{-\infty}^{+\infty}\mathrm{d}t_l \langle\Phi_0|T\Big\{\Omega_I(t_1)\ldots\Omega_I(t_l) A^{g_1}_{I\,a}(t) A^{g_2}_{I\,b}(t') A^{\dagger\,g_4}_{I\,d}(t'^{+}) A^{\dagger\,g_3}_{I\,c}(t^{+})\Big\}|\Phi_0\rangle_{\mathrm{C}}$$

$$+i\sum_{m=0}\left(\frac{-i}{\hbar}\right)^m \frac{1}{m!}\int_{-\infty}^{+\infty}\sum_{n=0}\left(\frac{-i}{\hbar}\right)^n \frac{1}{n!}\left[\prod_{i=1}^{m}\int_{-\infty}^{+\infty}\mathrm{d}t_i\right]\left[\prod_{i=j}^{n}\int_{-\infty}^{+\infty}\mathrm{d}t_j\right]\langle\Phi_0|T\Big\{\Omega_I(t_1)\ldots\Omega_I(t_m) A^{g_1}_{I\,a}(t) A^{\dagger\,g_3}_{I\,c}(t^{+})\Big\}|\Phi_0\rangle_{\mathrm{C}}\langle\Phi_0|T\Big\{\Omega_I(t_1)\ldots\Omega_I(t_n) A^{g_2}_{I\,b}(t') A^{\dagger\,g_4}_{I\,d}(t'^{+})\Big\}|\Phi_0\rangle_{\mathrm{C}}\,,$$

where $|\Phi_0\rangle$ is the *g.s.* of the unperturbed grand-canonical potential $\Omega_U$. Time-ordered products are evaluated by means of Wick's theorem, converting them into fully-contracted normal-ordered products of second-quantization operators. Up to third order, these contributions have been generated, sorted and evaluated in time and energy representation by computer codes.

▶ Fully-contracted Wick's theorem contributions admit a graphical representation as Feynman diagrams. At order $l = m + n$, the latter are graphs with $m$ ($n$) one (two)-body vertices linked one another by $2n + m + 2$ unperturbed one-body propagators. Unperturbed (dressed) one-body propagators are depicted by single (double) oriented lines, whose direction depends on the Nambu indices. For the vertices, Abrikosov-Hügenholtz notation is adopted [20].

▶ The orientation of the propagators specifies the topology of the diagrams, whereas subgraphs of order $p \leq l$ in a Feynman diagram of order $l$ which can be isolated by cutting two propagation lines are dressings of order $p$. Diagrams devoid of arrows in the propagation lines are called *unoriented*.

▶ The fully-contracted terms obtained from the first term on the r.h.s. of the expansion formula at a given order in $\Omega_I$, can be classified into five categories, depending on their topology as Feynman diagrams. If the latter (do not) contain unliked subgraphs, they are called disjoint (conjoint) diagrams. When the unliked subgraph is not connected to any external leg, the diagram is disconnected, thus must be neglected [19].

The remaining disjoint diagrams consist of direct, exchange and Bogoliubov contributions. Conjoint diagrams possess at least a two-body vertex and are divided, in turn, into *skeleton* and *composite* graphs. Composite diagrams contain at least one vertex that can be reabsorbed as a dressing in one unperturbed one-body propagators. Otherwise, the diagram is of skeleton type.

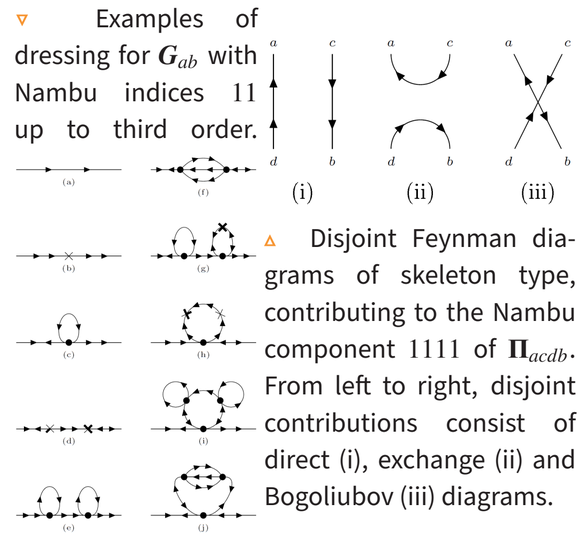


▵ Examples of dressing for $\boldsymbol{G}_{ab}$ with Nambu indices 11 up to third order. Disjoint Feynman diagrams of skeleton type, contributing to the Nambu component 1111 of $\boldsymbol{\Pi}_{acdb}$. From left to right, disjoint contributions consist of direct (i), exchange (ii) and Bogoliubov (iii) diagrams.

▶ Ispired by the ADG code in Ref. [21], the *automated implementation of Wick's theorem* (AIWT) code has been devised in C++, *Mathematica* and *Jupyter* [15]. At order $l = m + n$, the first term on the r.h.s. of the expansion formula delivers $4n + 2m + 3!!$ contributions, which are generated and sorted by category. Next, identical contributions are summed, whereas irrelevant fully-contracted terms are discarded. Then, the selected fully-contracted terms are evaluated and their corresponding expression in time representation is produced. Finally, for each of the $n + m + 2!$ Goldstone orderings of the time indices in the interaction and in the external points [17], the Fourier transform to energy representation is performed and the result of the integration returned.

▶ For the numerical calculation of the transition matrix elements and the energy eigenvalues of the excited states, it is convenient to adopt the algebraic diagrammatic construction scheme (ADC) [17, 10] and extend to Gorkov's formalism. The latter has been currently developed at order one (cf. ADC[1] in Ref. [22]), with one- and two body vertices, whereas the derivation of the ADC[2] scheme is in progress.

## The polarization propagator

▶ The polarization propagator is obtained from the two-time limit of the two-body response function [17], the latter being a function of the one-body propagator (4 elements), $\mathbf{G}_{ac}(t, t'')$, [1], and the two-body propagator (16 elements), $\mathbf{G}_{abcd}(t, t', t'', t''')$ [17]. In terms of the second quantization operators, the polarization propagator in time representation reads

$$\Pi^{g g'' g''' g'}_{acdb}(t, t') = -i\langle\Psi^A_0|T\Big\{A^{g}_a(t) A^{g'}_b(t') A^{\dagger\,g'''}_d(t'^{+}) A^{\dagger\,g''}_c(t^{+})\Big\}|\Psi^A_0\rangle$$
$$+i\langle\Psi^A_0|T\Big\{A^{g}_a(t) A^{\dagger\,g''}_c(t^{+})\Big\}|\Psi^A_0\rangle\langle\Psi^A_0|T\Big\{A^{g'}_b(t') A^{\dagger\,g'''}_d(t'^{+})\Big\}|\Psi^A_0\rangle\,.$$

▶ If the Schrödinger problem is time-independent, Lehmann's representation of Gorkov's polarization propagator can be decomposed into two interrelated parts,

$$\Pi^{g g'' g''' g}_{acdb}(\omega) \equiv \Pi^{+\,g g'' g''' g}_{acdb}(\omega) + \Pi^{-\,g g'' g''' g}_{acdb}(\omega)\,,$$

where the two contributions are related by complex conjugation [15], for example

$$\Pi^{+\,g g'' g''' g'}_{acdb}(\omega) = \sum_{k\neq 0}\frac{{}^{k}\chi^{g g''}_{ac}\ {}^{k}\chi^{*\,g''' g'}_{db}}{\omega - (\Omega_k - \Omega_0)/\hbar + i\eta}\,.$$

▶ The poles permits to access the excitation spectrum of the nucleus, whereas the residues associated with them are given by pairs of *transition matrix elements* [18],

$${}^{k}\chi^{g_1 g_2}_{bc} \equiv \langle\Psi_0|A^{g_1}_b A^{\dagger\,g_2}_c|\Psi_k\rangle\,,$$

$${}^{k}\Upsilon^{g_1 g_2}_{bc} \equiv \langle\Psi_k|A^{g_1}_b A^{\dagger\,g_2}_c|\Psi_0\rangle\,.$$

From the latter, one extracts EM multipole transition probabilities between the *g.s.* and excited states of the nucleus.

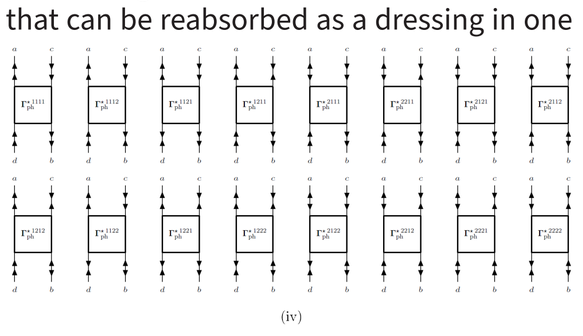


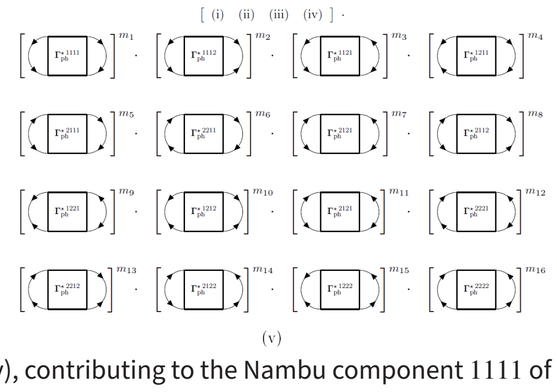


▵ Conjoint diagrams (iv) and disconnected diagrams (v), contributing to the Nambu component 1111 of the polarization propagator [15]. The insertions are elements the of *proper particle-hole vertex* [23].